Available on line www.jocpr.com

Journal of Chemical and Pharmaceutical Research

J. Chem. Pharm. Res., 2010, 2(5):656-681

ISSN No: 0975-7384
CODEN(USA): JCPRC5

Study of the optimized molecular structures and vibrational characteristics of neutral L-Ascorbic acid and its anion and cation using density functional theory

Priyanka Singh[a], N. P. Singh[a], R. A. Yadav[b]

[a]*Lasers and Spectroscopy Laboratory Department of Physics, U P (PG) Autonomous College, Varanasi, India*
[b]*Department of Physics, Banaras Hindu University, Varanasi, India*

ABSTRACT

FTIR spectra of the neutral L-Ascorbic acid (vitamin C) (L-AA) have been recorded in the range 50-4000 cm^{-1} on a Varian spectrometer model 3100 using KBr and Nujol optics with 2 cm^{-1} resolution. The computations were carried out by employing the RHF and DFT methods to investigate the optimized molecular geometries, atomic charges, thermodynamic properties and harmonic vibrational frequencies along with intensities in IR and Raman spectra and depolarization ratios of the Raman bands for the neutral L-AA and its singly charged anionic (L-AA^-) and cationic (L-AA^+) species. All the 54 normal modes of the L-AA molecule have been assigned and discussed in details in the present study. The bond lengths in the lactone ring for the 2 (C-O) bonds in L-AA^- are found to increase whereas for L-AA^+ these are found to be decrease as compared to the neutral molecule. The bond angles α(C-O-H) decreases in L-AA^- but increases for L-AA^+ as compared to the neutral molecule. The dihedral angle H-C-C-H increases by 12.4° while reverse change is noticed for the other H-C-C-H dihedral angle which decreases by 14.3° in going from L-AA to L-AA^- . The magnitudes of the calculated frequencies for the δ(C-H) modes ν_{38} and ν_{34} decrease by 37 and 27 cm^{-1} for L-AA^- whereas increase 15 and 33 cm^{-1} for L-AA^+ with respect to the neutral molecule. The radicalization of the neutral molecule shifts the magnitude of the frequency of the ν(C-OH) mode ν_{32} by ~30 cm^{-1} for L-AA^- and by 20 cm^{-1} for L-AA^+ and the IR intensity for the ν_{32} mode decreases in going from L-AA to L-AA^- to L-AA^+.

Keywords: *ab initio* and DFT studies; optimized molecular geometries; APT charges; vibrational characteristics; Ascorbic Acid (L-AA) and its singly charged radical anion and cation of L-ascorbic acid.

INTRODUCTION

L-Ascorbic acid (also called vitamin C), hereafter abbreviated as L-AA; is one of the most essential vitamins for both pharmaceutical and food processing industries. In view of its nutritional significance, varied uses in food and high daily doses necessary for optimum health, L-AA is a very significant vitamin for better public health [1]. It has been reported that large doses of vitamin C increases greatly the rate of production of lymphocytes under antigenic stimulation and it is well established that such a high rate of lymphocyte blastomogenesis is associated with a favourable prognosis of cancer [2-9]. L-AA is known to kill HIV-positive cells and to be useful in HIV-positive patients as a consequence of the potentiating the immune system [10].

L-AA is a six-carbon keto-lactone, a strong reducing agent and serves as an antioxidant. The hydrogen donation from L-AA is considered to be primarily responsible for the antioxidant properties attributed to this molecule. It contains four OH groups (two enol OH groups on lactone ring carbons and two OH groups on the side chain C atoms). It can be very easily oxidized and changed to dehydroascorbic acid. Its four hydroxyl (OH) groups play important role in its antioxidant property.

The crystal structure of this compound was studied by different workers [11-13]. Al-Laham et al. [14] performed conformational analysis of AA by forcing geometry of the ring to be constant and optimizing only the conformers of the side chain while Mora and Melendez [15] optimized 36 conformers of AA at the RHF/6-31G, RHF/6-31G(d,p), RHF/6-311+G(d,p) and MP2/6-31G(d,p) levels. The fully optimized gas phase structure [15] was found to be closer to the so called crystallographic B structure of L-AA molecule. The structural and vibrational studies of the L-AA molecule were carried out by number of workers [16-21]. We have recently [22] made a comprehensive structural and vibrational studies of this molecule using DFT and ab initio methods and the reported experimental structural and vibrational spectral data.

In the present paper the optimized geometries, APT charges, thermodynamic properties and harmonic vibrational frequencies along with their IR intensities and Raman activities and depolarization ratios of the Raman lines of singly charged positive and negative radicals of the L-AA molecule have been computed and the results for the neutral L-AA molecule and its anion and cation are compared.

EXPERIMENTAL SECTION

The compound L-Ascorbic acid (L-AA) was purchased from Sigma-Aldrich Chemical Company, (USA) with a purity ≥ 99%. This is a white solid at room temperature. It was used as such without further purification for recording the spectra. IR spectra have been recorded in KBr pellets and Nujol mull using Varian FTIR-3100 spectrometer in the spectral range 50-4000 cm^{-1} with the following experimental parameters:

Varian FTIR-3100: scans – 200; resolution – 2 cm^{-1}; gain – 50. The recorded IR and Far IR for the neutral L-AA molecule are reproduced in Figs. 1 and 2 respectively.

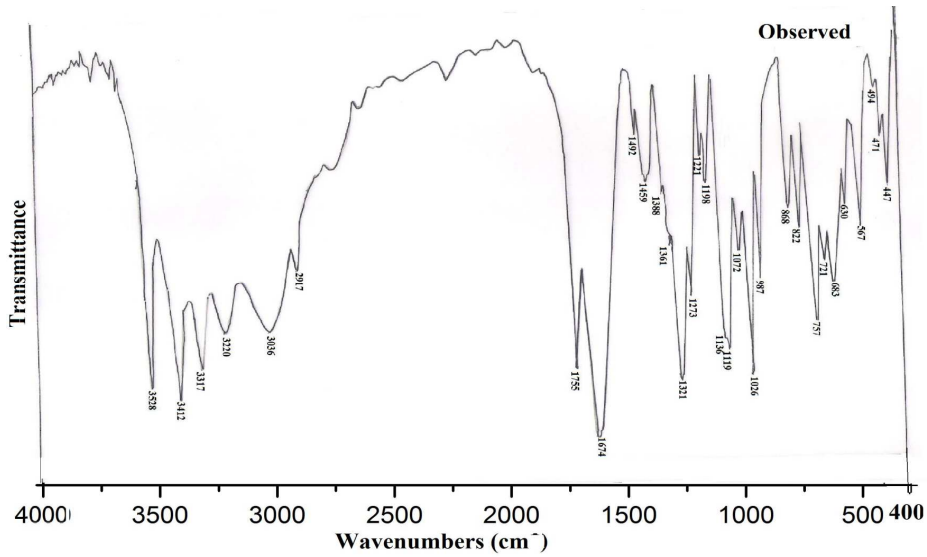

Fig.-1. Experimental FTIR spectrum of L-AA in KBr pellet/Nujol mull

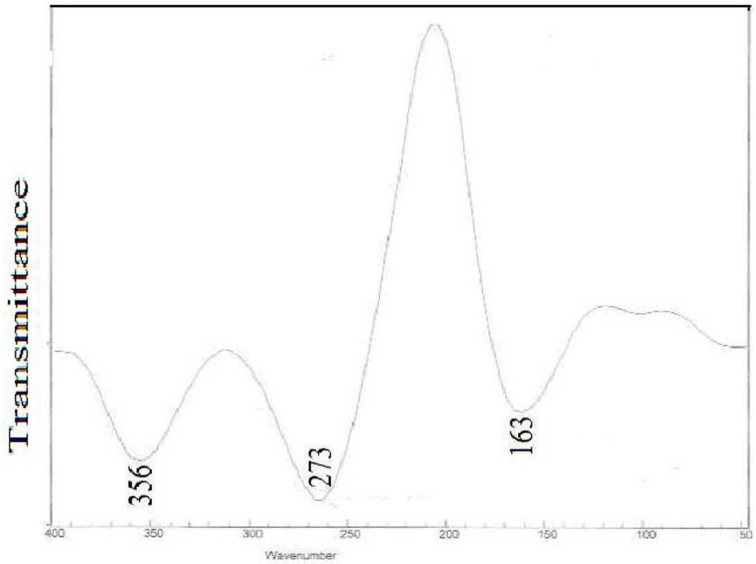

Fig.-2. Experimental Far IR spectrum of L-AA in KBr pellet/Nujol mull

Theoretical Computations

ab initio and DFT computations of the molecular structures, atomic charges and vibrational frequencies along with the corresponding IR intensities and Raman activities and depolarization ratios of the Raman bands were carried out for L-AA and its singly charged cationic and anionic radicals under the present study employing the RHF/6-31+g* and B3LYP/6-311++G** methods with the help of the Gaussian 03 package [23]. The geometry optimization and computation of the different quantities for the neutral L-AA molecule were carried out as detailed elsewhere [22]. For the anion radical the optimized geometry of the neutral molecule was taken as the input structure and calculations were performed by taking the charge as -1 and multiplicity as 2. Similarly, for the computations for the cation radical, the optimized geometry of the neutral

molecule was taken as the input structure and the calculations were performed by taking the charge as +1 and multiplicity as 2. The assignments of the normal mode of vibration for the neutral molecule and its radical anion and cation species were made by visual inspection of the individual mode using the Gauss View software [24]. The observed IR frequencies corresponding to the fundamental modes have been correlated to the calculated fundamental frequencies.

RESULTS AND DISCUSSION

4.1. Molecular structures

The optimized geometrical structures for the L-AA molecule and its radical anion and cation calculated at the B3LYP/6-31++G** level along with the experimental parameters are collected in Table-1. The atomic numbering for these molecules are shown in Figs 3-5. As expected the neutral molecule and its radical anion and cation possess non-planar structures with C_1 point group symmetry.

As can be seen from the Table-1, the optimized bond lengths of the two single C-C bonds, C_1-C_5 and C_3-C_4 in the lactone ring are calculated to be 1.499 Å and 1.457 Å respectively for the neutral molecule. For the neutral molecule shortening of the C_3-C_4 bond as compared to the C_1-C_5 bond is noticed which could be due to attachment of the O atom at the site C_3. For the molecule, the calculated values of all the four C-C bonds (including the lactone ring and the side chain) are found to agree with the corresponding experimental values [18] within 0.002 Å - 0.005 Å. The two C-O bond lengths C_1-O_2 and O_2-C_3 in the lactone ring are found to be ~1.45 Å and 1.37 Å. In this case also the shorter bond length r (O_2-C_3) as compared to the bond length r(C_1-O_2) is a consequence of the attachment of the O atoms at the site C_3. The bond length r (C_5-O_9) has slightly reduced value for the neutral molecule containing OH group(s). However, there is no such difference for the bond length r(C_4-O_7). The r(C_1-H_{11}) and r(C_{12}-H_{13}) bond lengths appear to be unaffected due to substitution as long as there is at least two identical C-H bonds attached to the site C_1/C_{12}. All the four calculated O-H bond lengths are found to agree with the corresponding experimental values [18] within 0.017 Å – 0.039 Å. The bond angles α(O_2-C_1-C_5) and α(O_2-C_3-C_4) are found to be 103.9° and 108.3° respectively, whereas the α(C_3-C_4-O_7) and α(C_4-C_5-O_9) are found to be 123.1° and 131.3° respectively.

No experimental data for the geometrical structures for radical ions are available. In the L-AA^- species due to addition of an electron, the oxygen atom strongly pulls the electron cloud of other atoms towards itself in the lactone ring. The ab initio electron density analysis shows that the removal of electron is delocalized mostly in the ring portion of the radical cation (L-AA^+). This is reflected in the relative changes of the bond distances as well as bond angles in both the radical ions as compared to the neutral molecule. The calculated bond length r(C_4-C_5) of L-AA^- (0.052 Å) and L-AA^+ (0.065 Å) is longer than those of the L-AA molecule. The calculated bond length in the lactone ring r(C_1-C_5) and r(O_2-C_3) increase in going from L-AA to L-AA^- by ~0.31 Å and decrease in going from L-AA to L-AA^+ by ~0.046 Å. Both the carbonyl bond lengths r(C_4-O_7) and r(C_5-O_9) of L-AA^- are increased whereas for L-AA^+ these are found to decrease as compared to the neutral molecule. As a result, the bond angles α(O_2-C_1-C_{12}), α(H_{11}-C_1-C_{12}) and α(O_2-C_3-O_6) increase in L-AA^- but in decrease L-AA^+ as compared to the neutral molecule

whereas the bond angle $\alpha(O_2\text{-}C_3\text{-}C_4)$ decreases in both radical ions as compared to the neutral molecule.

It can be seen from the Table-1, which all the dihedral angles of the lactone moiety (consisting of atoms C_1 to H_{10}) are found to be either ± 0° or ±180° within ±0.03°. The value of the dihedral angles $C_1\text{-}C_{12}\text{-}C_{16}\text{-}H_{17}/C_1\text{-}C_{12}\text{-}C_{16}\text{-}H_{18}$ increase considerably (14.1°/12.2°) in going from the L-AA to L-AA^- molecules whereas these decrease by 8.2°/8.7° in going from the L-AA to L-AA^+ molecules due to the attachment of an OH group at the site C_{13}. The dihedral angle $O_{14}\text{-}C_{12}\text{-}C_{16}\text{-}H_{17}$ increases slightly (by 1.9°) while the angle $O_{14}\text{-}C_{12}\text{-}C_{16}\text{-}H_{18}$ decreases considerably by 13.8° in going from the L-AA to L-AA^- molecules. However, the magnitude of the dihedral angle $O_{14}\text{-}C_{12}\text{-}C_{16}\text{-}H_{17}/O_{14}\text{-}C_{12}\text{-}C_{16}\text{-}H_{18}$ is found to decrease by ~12.0° and increase by 12.5° in going from the L-AA to L-AA^+ molecules. The value of the dihedral angles $C_{16}\text{-}C_{12}\text{-}O_{14}\text{-}H_{15}$ and $H_{13}\text{-}C_{12}\text{-}O_{14}\text{-}H_{15}$ increase in going from L-AA to L-AA^- and decreases in going from L-AA^- to L-AA molecules. The magnitude of the dihedral angle $H_{13}\text{-}C_{12}\text{-}C_{16}\text{-}H_{18}$ increases by 12.4° while reverse effect is calculated for the dihedral angles $C_1\text{-}C_{12}\text{-}C_{16}\text{-}O_{19}$ and $H_{13}\text{-}C_{12}\text{-}C_{16}\text{-}H_{17,}$ which decrease by 15.4° and 14.3° respectively, in going from the L-AA to L-AA^- while the value of the dihedral angles $C_1\text{-}C_{12}\text{-}C_{16}\text{-}O_{19}$ and $H_{13}\text{-}C_{12}\text{-}C_{16}\text{-}H_{17}$ increases in going from the L-AA^- to L-AA^+. Different bond lengths, bond angles and dihedral angles along with their values are shown in figs. 6(a), 6(b) and 6(c), respectively, for the three molecules L-AA, L-AA^- and L-AA^+. It can be seen from fig. 6(a) that there is variation in the bond lengths for (seven bonds) only due to radicalization. However, in bond angles (Fig. 6b) and dihedral angles (Fig. 6c) variations are noticeable for many more cases.

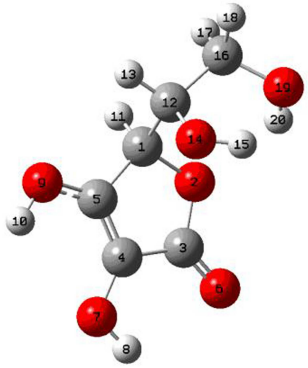

Fig.-3: L-AA

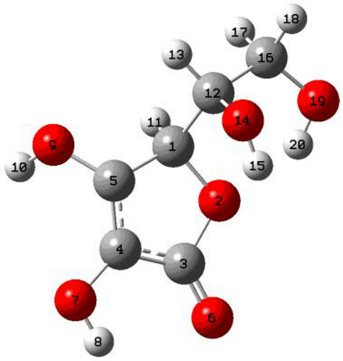

Fig.- 4: L-AA^-

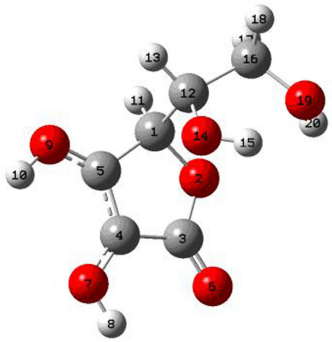

Fig.-5: L-AA$^+$

Figures: 3-5. Atomic labeling scheme for L-AA and its radical ions

Table-1: Computed and experimental geometrical parameters[b] of L-AA and its radical ions

Parameters	L-AA		L-AA$^-$	L-AA$^+$
	Cal.	Obs[c].	Cal.	Cal.
r(C_1-O_2)	1.450	1.444	1.450	1.451
r(C_1-C_5)	1.499	1.491	1.506	1.496
r(C_1-H_{11})	1.096	1.011	1.112	1.093
r(C_1-C_{12})	1.543	1.521	1.538	1.560
r(O_2-C_3)	1.377	1.355	1.432	1.351
r(C_3-C_4)	1.457	1.452	1.405	1.493
r(C_3-O_6)	1.204	1.216	1.236	1.193
r(C_4-C_5)	1.340	-	1.392	1.405
r(C_4-O_7)	1.355	1.361	1.386	1.293
r(C_5-O_9)	1.343	1.326	1.396	1.291
r(O_7-H_8)	0.968	0.929	0.968	0.981
r(O_9-H_{10})	0.966	0.949	0.975	0.975
r(C_{12}-C_{16})	1.538	1.521	1.535	1.546
r(C_{12}-H_{13})	1.096	1.137	1.097	1.096
r(C_{12}-O_{14})	1.413	1.427	1.422	1.408
r(O_{14}-H_{15})	0.968	0.937	0.966	0.973
r(C_{16}-H_{17})	1.097	1.107	1.103	1.094
r(C_{16}-H_{18})	1.091	1.065	1.094	1.092
r(C_{16}-O_{19})	1.424	1.431	1.424	1.417
r(O_{19}-H_{20})	0.967	0.945	0.970	0.964
α(O_2-C_1-C_5)	103.9	104.2	105.0	104.4
α(O_2-C_1-H_{11})	107.4	-	108.5	108.5
α(O_2-C_1-C_{12})	110.3	-	107.7	110.0

α(C_5-C_1-H_{11})	111.1	110.5	109.0	112.5
α(C_5-C_1-C_{12})	114.9	114.8	118.7	109.6
α(H_{11}-C_1-C_{12})	109.0	110.6	107.6	111.6
α(C_1-O_2-C_3)	109.5	109.5	108.2	111.8
α(O_2-C_3-C_4)	108.3	109.5	107.2	107.4
α(O_2-C_3-O_6)	123.6	121.4	120.8	127.5
α(C_4-C_3-O_6)	128.1	129.1	131.7	125.1
α(C_3-C_4-C_5)	108.8	107.8	111.7	107.9
α(C_3-C_4-O_7)	123.1	124.6	121.1	125.3
α(C_5-C_4-O_7)	128.1	127.5	126.7	126.8
α(C_1-C_5-C_4)	109.5	109.5	105.4	107.7
α(C_1-C_5-O_9)	119.3	116.9	117.4	121.8
α(C_4-C_5-O_9)	131.3	133.7	125.6	130.4
α(C_4-O_7-H_8)	108.0	106.1	105.0	111.3
α(C_5-O_9-H_{10})	109.8	117.7	108.7	114.2
α(C_1-C_{12}-C_{16})	111.9	112.7	111.9	113.4
α(C_1-C_{12}-H_{13})	106.2	108.1	106.9	106.0
α(C_1-C_{12}-O_{14})	111.6	107.6	112.1	107.5
α(C_{16}-C_{12}-H_{13})	109.0	-	107.4	109.4
α(C_{16}-C_{12}-O_{14})	110.4	106.9	111.4	111.0
α(H_{13}-C_{12}-O_{14})	107.5	-	106.7	109.3
α(C_{12}-O_{14}-H_{15})	106.8	109.0	106.7	107.3
α(C_{12}-C_{16}-H_{17})	110.6	108.1	108.1	111.5
α(C_{12}-C_{16}-H_{18})	109.0	107.4	108.8	107.5
α(C_{12}-C_{16}-O_{19})	111.4	108.0	114.8	110.3
α(H_{17}-C_{16}-H_{18})	108.3	108.7	107.9	108.2
α(H_{17}-C_{16}-O_{19})	111.7	107.3	110.5	112.7
α(H_{18}-C_{16}-O_{19})	105.7	110.7	106.5	106.3
α(C_{16}-O_{19}-H_{20})	108.3	110.5	107.8	110.9
δ(H_{11}-C_1-O_2-C_3)	119.4	-	103.0	129.6
δ(C_{12}-C_1-O_2-C_3)	122.0	-	140.8	108.1
δ(H_{11}-C_1-C_5-C_4)	116.3	-	100.5	125.9
δ(H_{11}-C_1-C_5-O_9)	64.0	-	44.9	57.3
δ(C_{12}-C_1-C_5-C_4)	119.4	-	136.0	109.3
δ(C_{12}-C_1-C_5-O_9)	60.3	-	78.6	67.5
δ(O_2-C_1-C_{12}-C_{16})	56.1	-	67.3	57.2
δ(O_2-C_1-C_{12}-H_{13})	175.0	-	175.4	177.2
δ(O_2-C_1-C_{12}-O_{14})	68.1	-	58.8	65.9
δ(C_5-C_1-C_{12}-C_{16})	173.0	-	173.7	171.4

δ(C_5-C_1-C_{12}-H_{13})	68.1	-	56.3	68.6
δ(C_5-C_1-C_{12}-O_{14})	48.8	-	60.2	48.3
δ(H_{11}-C_1-C_{12}-C_{16})	61.6	-	49.5	63.3
δ(H_{11}-C_1-C_{12}-H_{13})	57.3	-	67.9	56.8
δ(H_{11}-C_1-C_{12}-O_{14})	174.2	-	175.5	173.6
δ(C_1-C_5-O_9-H_{10})	175.5	-	112.3	174.7
δ(C_4-C_5-O_9-H_{10})	4.0	-	25.4	1.2
δ(C_1-C_{12}-O_{14}-H_{15})	94.4	-	37.7	109.0
δ(C_{16}-C_{12}-O_{14}-H_{15})	30.8	-	88.7	15.6
δ(H_{13}-C_{12}-O_{14}-H_{15})	149.5	-	154.4	136.4
δ(C_1-C_{12}-C_{16}-H_{17})	46.3	-	60. 4	38.1
δ(C_1-C_{12}-C_{16}-H_{18})	165.2	-	177.4	156.5
δ(C_1-C_{12}-C_{16}-O_{19})	78.7	-	63.3	88.0
δ(H_{13}-C_{12}-C_{16}-H_{17})	70.9	-	56.6	80.0
δ(H_{13}-C_{12}-C_{16}-H_{18})	48.0	-	60.4	38.4
δ(H_{13}-C_{12}-C_{16}-O_{19})	164.3	-	179.6	154.0
δ(O_{14}-C_{12}-C_{16}-H_{17})	171.2	-	173.1	159.2
δ(O_{14}-C_{12}-C_{16}-H_{18})	69.9	-	56.1	82.4
δ(O_{14}-C_{12}-C_{16}-O_{19})	46.3	-	63.1	33.2
δ(C_{12}-C_{16}-O_{19}-H_{20})	65.5	-	35.3	93.2
δ(H_{17}-C_{12}-O_{19}-H_{20})	58.7	-	87.2	32.2
δ(H_{18}-C_{16}-O_{19}-H_{20})	176.2	-	155.8	150.6

b: Bond lengths(r) in Angstrom as (Å), bond angles(α) and dihedral angles(δ) in degrees as (°). c: Ref. [28]

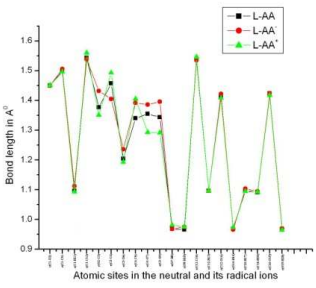

Fig.-6(a)

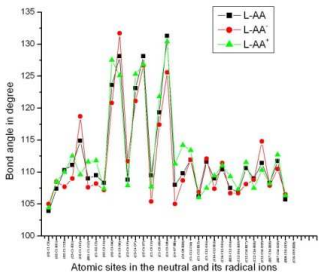

Fig.-6(b)

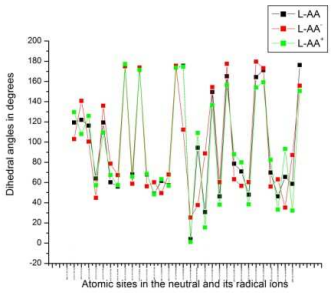

Fig.-6(c)

Figs. 6(a-c): The bond lengths, bond angles and dihedral angles differences from theoretical approaches of the neutral L-AA molecule and its radical ions.

Atomic Charges

APT charges at the various atomic sites of the neutral L-AA molecule and its radical ions calculated are collected in Table-2. The calculated atomic charges at different atomic sites are plotted in Fig.-7 for the neutral molecule and its radical ions. L-AA is a dibasic acid with an

enediol group built into a five membered heterocyclic lactone ring. The molecule is stabilized by delocalization of the π-electron over the conjugated carbonyl and enediol system. All the oxygen atoms are seen to possess negative charges due to their electron-withdrawing nature. However, for the lactone ring, the O_2 and O_7 atom(s) the value of the charges decrease by -0.1100 and -0.0674 in L-AA^- and by -0.1406 and -0.0399 in L-AA^+ as compared to the neutral molecule. The APT charges at the sites O_{14} and O_{19} increase in going from the L-AA^+ to L-AA^- and L-AA^+ to L-AA due to radicalization. In the lactone ring, all the four C atoms possess positive charges but in L-AA^-, C_4 and C_5 are negative because they are strongly affected by bond character. The maximum positive charge on the atom C_3 due to presence of the two electronegative O atoms attached to the C_3 site. The charge at the sites C_{12} and C_{13} decrease in going from L-AA to L-AA^- by 0.0523/0.0261 but increases by 0.0836/0.0187 in going from L-AA^- to L-AA^+ due to radicalization. For the neutral and anionic species, the increasing magnitude of charge on the carbon atoms of the side chain in the order $C_{13}>C_{12}$ due to the attachment of the hydroxyl group while as a result of cationic radicalization of L-AA, the charges are found to be in the reverse order i.e, $C_{13}<C_{12}$.

The charges computed for the H_8 and H_{10} atoms are found to be decrease in going from the neutral species to the anionic species whereas these increase in going from the anionic species to cationic species due to the bond character (see, Figs. 3-5). The charge is more negative in the anionic species and less negative in the cationic species at the sites H_{17}/H_{18} as compared to the neutral species. Thus, in the case of electron addition the most of the negative charge is concentrated at the O_{19} atom. The charge at the site H_{15} decreases by -0.0210 in going from the neutral species to the anionic species while increases by 0.0364 in going from the anionic to the cationic species. However, reverse effect is observed at the site H_{20}, whose charge increases by 0.0208 in going from the L-AA to L-AA^- and decreases by -0.0149 in going from the L-AA to L-AA^+ species.

Table - 2: Calculated APT charges at various atomic sites for L-AA and its radical ions

Atoms	L-AA	L-AA^-		L-AA^+	
	APT charges q	APT charges q^-	$\Delta q = q^- - q$	APT charges q^+	$\Delta q = q^+ - q$
C_1	0.2858	0.4511	0.1653	0.0193	-0.2665
O_2	-0.7618	-0.6581	0.1100	-0.6212	0.1406
C_3	1.2806	1.7394	0.4588	1.0167	-0.2639
C_4	0.0861	-0.2124	-0.2985	0.4323	0.3462
C_5	0.5882	-0.4218	-1.0100	0.8161	0.2279
O_6	-0.8662	-1.4211	-0.5549	-0.6141	0.2521
O_7	-0.6427	-0.5753	0.0674	-0.6028	0.0399
H_8	0.3355	0.2270	-0.1085	0.4202	0.0847
O_9	-0.7100	0.2402	0.9502	-0.6734	0.0366
H_{10}	0.3072	-0.1674	-0.4746	0.4036	0.0964
H_{11}	-0.0311	-0.1978	-0.1667	0.0748	0.1059
C_{12}	0.4116	0.3593	-0.0523	0.4429	0.0313
H_{13}	-0.0241	-0.0376	-0.0135	-0.0194	0.0047

O_{14}	-0.5992	-0.5729	0.0263	-0.5567	0.0425
H_{15}	0.2969	0.2759	-0.0210	0.3333	0.0364
C_{16}	0.4211	0.3950	-0.0261	0.4137	0.0094
H_{17}	-0.0523	-0.0713	-0.0190	-0.0085	0.0438
H_{18}	-0.0175	-0.0534	-0.0359	0.0137	0.0312
O_{19}	-0.6142	-0.6256	-0.0114	-0.5819	0.0323
H_{20}	0.3063	0.3271	0.0208	0.2914	-0.0149

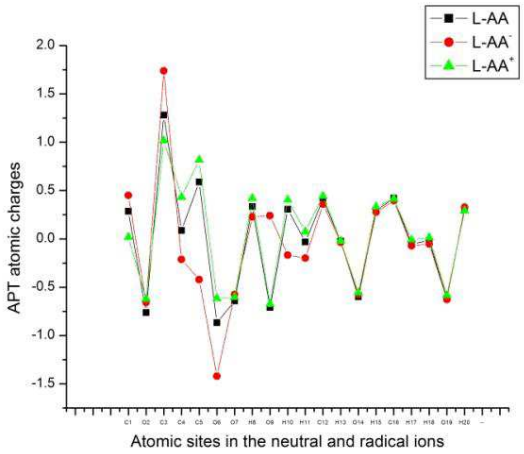

Fig. 7: APT atomic charges at various atoms of the L-AA molecules and its radical ions.

Vibrational Assignments

Neutral Molecule

The computed IR and Raman spectra for the neutral L-AA molecule and its radical ions are shown in Figs. 8-13. The calculated fundamental frequencies along with their IR intensities, Raman activities, depolarization ratios for the Raman bands and the proposed vibrational assignments are collected in Table-3. The experimentally observed FTIR frequencies for the neutral molecule are also included in the Table-3. The normal mode assignments were made with the help of Gauss View software. In order to make consistent assignments for all the fundamental modes of the L-AA molecule help has been taken from the normal mode assignments made for the DHF, DHMF, DHHMF and DHHEF molecules [22], calculated IR intensities and Raman activities as well as the Raman depolarization ratios along with the experimental IR and Raman spectral studies [18-21] for the L-AA molecule.

There are several inconsistencies in the assignments of the fundamentals of the neutral L-AA molecule [18-21]. Dimitrova [18] distributed the 54 normal modes of L-AA as: the torsional modes-16; the deformation modes-19 and the stretching modes-19 whereas Panicker et al.[19] have assigned only thirty-eight normal modes based on their FT-IR, FT-Raman and SERS spectral studies. Obviously the distribution reported earlier [19] is incorrect and that given by Panicker et al. is incomplete. As the L-AA molecule is a twenty-atomic molecule, its 54 normal modes of vibration are : 20-stretching modes (ν) corresponding to the twenty bonds, 8-deformation modes (δ) as the 2 $\delta(C_1\text{-}C_{12})$, 2 $\delta(C_{12}\text{-}C_{16})$, 2 $\delta(C_1\text{-}H_{11})$ and 2 $\delta(C_{12}\text{-}H_{13})$ modes, 8-

angle bending modes (α) as the 4 α(C-O-H),2 α(C-C-O) and 2 angle bending of the lactone ring, 3-in–plane (with respect to the lactone ring) bending modes (β) as the 2 β(C-OH) and 1 β(C=O), 5-out-of plane (with respect to lactone ring) modes (γ/ϕ) as the 2 γ(C-OH), 1 γ(C=O) and 2 out-of plane lactone ring deformation ϕ, 7-torsional modes (τ) as the 4 τ(C-OH), 1 τ(CH_2), 1 τ(C_1-C_{12}) and 1 τ(C_{12}-C_{14}), 1-CH_2 scissoring mode (σ), 1-CH_2 rocking mode (ρ) and 1-CH_2 wagging mode (ω). As this molecule possesses C_1 symmetry all of its 54 normal modes of vibration are IR as well as Raman active.

O-H modes (12 modes)

There are 4 ν(OH), 4 α(C-O-H) and 4 τ(C-OH) modes due to the four OH groups two being attached to the ring and two to the side chain. The modes ν_{54}, ν_{53}, ν_{52}, ν_{51}, ν_{43}, ν_{42}, ν_{41}, ν_{35}, ν_{15}, ν_{14}, ν_{13} and ν_{11} correspond to these modes.

For the L-AA molecule the O-H stretching region exhibits four strong IR bands in the region 3216 cm^{-1} - 3626 cm^{-1} [18-19]. In the present case the recorded IR spectra contain four strong bands in the range 3200-3600 cm^{-1}, namely, 3220 (vs), 3317(vs), 3412(vs) and 3528(vs) cm^{-1}. The first three frequencies agree with the earlier reported frequencies [28-29], however, the fourth frequency agrees only with that reported by Panicker et al.[18]. The ν(O_9-H_{10}) mode is found to have higher frequency than the mode ν(O_7-H_8) which can be explained as follows: the H_{10} atom is hydrogen bonded with the O_7 atom whereas the H_8 atom is hydrogen bonded with the O_6 atom. Since the O_6 atom bears more negative charge as compared to the O_7 atom, the $O_{6...}H_8$ distance is smaller than the $O_{7...}H_{10}$, as a consequence of which the distance r(O_9-H_{10}) is larger than the distance r(O_7-H_8) giving rise to higher force constant corresponding to ν(O_9-H_{10}) as compared to that corresponding to ν(O_7-H_8). Similarly, the frequency ν(O_{19}-H_{20}) is higher than the frequency ν(O_{14}-H_{15}) which could be due to more negative charge on O_{19} as compared to that on the O_{14} atom. Thus, on the basis of APT charges only the order of frequencies of the four OH stretching modes should be ν(O_7-H_8) < ν(O_9-H_{10}) < ν(O_{14}-H_{15}) < ν(O_{19}-H_{20}). However, the four ν(O-H) modes of the L-AA molecule are found in the order ν(O_9-H_{10}) > ν(O_{19}-H_{20})>ν(O_7-H_8)>ν(O_{14}-H_{15}) (see Table-3, ν_{51}-ν_{54}) which could be due to complexity of hydrogen bonding in the lactone ring and the side chain. The presently observed frequencies 3220 (vs), 3317(vs), 3412(vs) and 3528(vs) cm^{-1} are correlated to the modes ν(O_9-H_{10}), ν(O_{19}-H_{20}),ν(O_7-H_8) and ν(O_{14}-H_{15}) respectively.

The ν_{11}, ν_{13}, ν_{14} and ν_{15} modes correspond to the four τ(OH) modes. Assignment of these τ(OH) modes is a difficult task as these are strongly coupled amongst themselves and with many other modes. The lowest magnitude (357 cm^{-1}) mode ν_{11} is found for the τ(O_7-H_8) mode which is coupled with the τ(O_9-H_{10}) mode with the corresponding IR frequency 356 cm^{-1} observed with very strong intensity. Earlier [17] this mode was correlated to the observed frequency at 350 cm^{-1}. The τ(O_9-H_{10}) mode is calculated to be 420 cm^{-1} and appears to be coupled with the τ(O_7-H_8) mode. The observed IR frequency 366 cm^{-1} was earlier correlated to this mode by Hvoslef [17], which seems to be quite a low frequency for this mode. No observed frequency could be correlated to this mode in the present case. The τ(O_{14}-H_{15}) mode, strongly coupled with the τ(O_{19}-H_{20}) and τ(O_9-H_{10}) modes has a magnitude of 424 cm^{-1}. The calculated frequency for the τ(O_{19}-H_{20}) mode is 524 cm^{-1} and this mode is strongly coupled with the τ(O_{14}-H_{15}) mode. The

observed frequencies corresponding to the OH torsional modes ν_{14} and ν_{15} have magnitudes 447 cm^{-1} and 494 cm^{-1} and appear to have medium and very weak IR intensities respectively.

Assignment of the angle bending modes α(C-O-H) is also complicated by coupling of these modes amongst themselves and with other modes. The mode ν_{35} arises due to $\alpha(C_4\text{-O-H})$ and is calculated to be 1302 cm^{-1} with the corresponding observed Raman and IR frequencies at 1258 cm^{-1} and 1246 cm^{-1} [19], respectively and it appears to be strongly coupled with the $\nu(C_5\text{-OH})$, $\delta(C_1\text{-}H_{11})$ and $\delta(C_{12}\text{-}H_{13})$ modes. The mode ν_{43} originates due to $\alpha(C_5\text{-O-H})$ and is strongly coupled with $\alpha(C_4\text{-O-H})$ mode and is calculated to have the frequency 1448 cm^{-1} which could be correlated to the observed IR frequency 1443(m) in agreement with the earlier [17] work. The angle bending mode ν_{41} arising due to $\alpha(C_{12}\text{-O-H})$ shows coupling with the $\delta(C_{12}\text{-}H_{13})$ mode and it is calculated to have a magnitude 1415 cm^{-1} with the corresponding observed frequency 1388 cm^{-1} in the IR spectrum. The $\alpha(C_{16}\text{-O-H})$ mode (ν_{42}) with the calculated frequency 1431 cm^{-1} and coupled with the $\alpha(C_{12}\text{-O-H})$ mode was earlier [19] correlated to the observed IR frequency 1385 cm^{-1} by which seems to be relatively a lower magnitude. No experimental frequency could be observed corresponding to this mode in the present case.

CH_2 modes (6 modes)

The CH_2 group has six normal modes of vibration as: an anti-symmetric stretching mode-$\nu_{as}(CH_2)$, a symmetric stretching mode-$\nu_S(CH_2)$, a scissoring mode-$\sigma(CH_2)$, a wagging mode-$\omega(CH_2)$, a torsional mode-$\tau(CH_2)$ and a rocking mode-$\rho(CH_2)$. The modes ν_{50}, ν_{47}, ν_{44}, ν_{39}, ν_{33} and ν_{26} correspond respectively to these modes. The CH_2 anti-symmetric and symmetric stretching modes (ν_{50} and ν_{47}) do not couple with any other modes, except the $C_1\text{-}H_{11}$ stretching mode which couples with the $\nu_S(CH_2)$ mode. Panicker et al. [19] observed three frequencies each in the IR (3030, 2917 and 2907 cm^{-1}) and Raman (3004, 2919 and 2879 cm^{-1}) spectra in the range 2850-3150 cm^{-1} corresponding to the C-H/CH_2 stretching modes; however, they did not correlate these frequencies to specific modes arising due to the C-H/CH_2 stretching modes. Dimitrova [18] correlated all the four C-H/CH_2 stretching frequencies to a single frequency observed at 2915 cm^{-1} and labeled the four C-H stretching modes as pure single bond C-H stretching modes [18]. The present calculations place the four C-H/CH_2 stretching frequencies at 3100, 3046, 3034 and 3011 cm^{-1} the first (3100 cm^{-1}) and the last (3011 cm^{-1}) frequencies of the above four correspond to the modes $\nu_{as}(CH_2)$ and $\nu_s(CH_2)$ while the second (3046 cm^{-1}) and third (3034 cm^{-1}) frequencies arise due to the in-phase (ip) and out-of-phase (op) coupling of the $C_{12}\text{-}H_{13}$ and $C_1\text{-}H_{11}$ stretching modes. As the calculated frequencies corresponding to the $\nu_{as}(CH_2)$ and $\nu_s(CH_2)$ modes differ by ~90 cm^{-1}, the frequencies 3030 cm^{-1} and 2879 cm^{-1} could be correlated to these modes. In the present case the observed frequency 3036 cm^{-1} is found to appear strongly in the IR spectra and could be correlated to the $\nu_{as}(CH_2)$ mode.

The calculated frequency 1501 cm^{-1} corresponding to the CH_2 scissoring mode (ν_{44}) is found to have very weak IR and Raman intensities and therefore, the observed frequencies 1487 and 1484 cm^{-1} with weak IR and Raman intensities [19] are correlated to this mode of L-AA molecule. The calculated frequency 1374 cm^{-1} with extremely weak intensities in the IR and Raman spectra respectively corresponding to the CH_2 wagging mode (ν_{39}) is coupled with the $\alpha(C_4\text{-O-H})$ mode,

which could be correlated to the observed [19] frequency 1364 cm^{-1} in the IR spectrum. The CH_2 torsion mode (ν_{33}) is calculated to be 1221 cm^{-1} with medium and weak intensities in the IR and Raman spectra, respectively, corresponding to the observed frequencies 1199 (s) and 1193 (w) cm^{-1} in the IR and Raman spectra [19]. The calculated frequency 964 cm^{-1} corresponding to the CH_2 rocking mode (ν_{26}) is found to have medium and very weak IR and Raman intensities, respectively, which could be correlated to the observed [19] frequencies 990 (s) cm^{-1} in the IR and 984 (w) cm^{-1} in the Raman spectra. From the present IR spectral study the IR bands are seen at 1492, 1361, 1198 and 987 cm^{-1} are correlated to the CH_2 scissoring, wagging, torsional and rocking modes with the corresponding correlated frequencies 1501, 1374, 1221 and 964 cm^{-1} respectively.

C-H modes (6 modes)

Stretching of the two C-H bonds C_1-H_{11} and C_{12}-H_{13} gives rise to two coupled C-H stretching modes as the in-phase(ip) coupled (ν_{48}) and out–of-phase(op) coupled (ν_{49}) C-H stretching modes which are calculated to be 3046 cm^{-1} and 3034 cm^{-1}. It is to be noted here that the ip and op coupled ν(C-H) modes should correspond to the $\nu_s(CH_2)$ and $\nu_{as}(CH_2)$ modes in magnitude, however, reverse of this is found in the present case which could be due to location of the C_1-H_{11} and C_{12}-H_{13} bonds at two different sites C_1 and C_{12}. As the two modes ν_{48} and ν_{49} have calculated frequencies lying between the frequencies due to the $\nu_{as}(CH_2)$ and $\nu_s(CH_2)$ modes, the observed frequencies due to the $\nu(C_1$-$H_{11})$ and $\nu(C_{12}$-$H_{13})$ modes should also lie between the observed frequencies due to the $\nu_{as}(CH_2)$ (3030 cm^{-1}) and $\nu_s(CH_2)$ (2879 cm^{-1}). Therefore, the frequencies 2915 cm^{-1} and 2907 cm^{-1} [17,19] are correlated to the two C-H stretching modes ν_{48} and ν_{49} respectively. The presently observed frequency 2917 cm^{-1} corresponds to the $\nu(C_1$-$H_{11})$ mode and has medium intensity in the IR spectra.

The present calculations place the two δ modes (ν_{40} and ν_{36}) due to the C_1-H_{11} bond at the frequencies 1388 and 1314 cm^{-1}, the former of which corresponds to the observed frequency ~1372 cm^{-1} [18, 19] while the latter one is coupled with the $\alpha(C_4$-OH) mode and corresponds to the observed IR frequency ~1276 cm^{-1} [17,19]. The remaining two δ modes (ν_{38} and ν_{34}) arising due to the C_{12}-H_{13} bond have calculated frequencies 1364 and 1240 cm^{-1} and are strongly coupled with the two $\delta(C_1$-$H_{11})$ modes. These modes (ν_{38} and ν_{34}) could be correlated to the observed frequencies 1344 cm^{-1} [17] and ~1221 cm^{-1} [17, 19]. In the present case the observed frequencies 1273 and 1221 cm^{-1} have been assigned to the modes ν_{36} and ν_{34} and these are found to appear with medium intensities in the IR spectra.

Lactone ring mode (9 modes)

The nine modes of vibration of the lactone ring are the five stretching modes - ν_{45}, ν_{30}, ν_{28}, ν_{27} and ν_{23}; two out-of-plane ring deformation modes - ν_{17} and ν_{18} and two in-plane ring deformation modes - ν_{20} and ν_{16}. Dimitrova [18] assigned five ring modes corresponding to the stretching vibrations whereas Panicker et al. [19] assigned only three ring modes corresponding to the stretching vibrations. The highest ring stretching mode ν_{45} corresponds to the C=C stretching mode and is calculated to be 1769 cm^{-1} which involves appreciable contribution from the C=O stretching also. The observed frequencies ~1670 cm^{-1} in the IR and Raman spectra [18, 19] could be correlated to the ν(C=C) mode which also agree with presently observed IR frequency 1674

cm^{-1}. The ring stretching mode ν_{30} involves mainly stretching of the O_2-C_3 bond and is calculated to be 1112 cm^{-1} corresponding to the observed frequency 1113 cm^{-1} [19]. This mode shows strong coupling of the ring stretching with the $\nu(C_4\text{-OH})$ and $\alpha(C_5\text{-OH})$ modes. The ring stretching mode ν_{28} with calculated frequency 1048 cm^{-1}, involves mainly stretching of the C_1-O_2 and C_3-O_2 bonds with slight contributions from the $\alpha(C_4\text{-OH})$ and $\alpha(C_5\text{-OH})$ modes. The observed frequency ~1045 cm^{-1} [19] could be assigned to the above mode. The ring stretching mode ν_{27} involves stretching of the C_1-C_5, C_3-C_4 and C_1-O_2 bonds and has the calculated frequency 1027 cm^{-1}. This mode is found to arise due to coupling of the ring stretching motions with the $\alpha(C_4\text{-O-H})$ and $\alpha(C_5\text{-O-H})$ modes. The observed IR and Raman frequencies at ~1025 cm^{-1} [17, 19] could be correlated to the mode ν_{27}. In the present case the experimentally observed frequency 1026 cm^{-1} in the IR spectrum is correlated to the mode ν_{27}. The last ring stretching mode ν_{23} having the calculated frequency 825 cm^{-1} is strongly coupled with the α(ring) mode corresponding to the observed IR and Raman frequencies at ~820 cm^{-1} [17, 19]. The IR frequency 822 cm^{-1} observed with medium intensity is correlated to the mode ν_{23}.

The planar-ring deformation mode ν_{18} is calculated to be 693 cm^{-1} with the corresponding observed frequency at ~690 cm^{-1} [19]. The other planar-ring deformation mode ν_{17} appears to arise due to ring deformation strongly coupled with the $\tau(O_{14}\text{-}H_{15})$ and $\tau(O_{19}\text{-}H_{20})$ modes and is found to have the frequency 564 cm^{-1}. The two non-planar ring deformation modes ν_{20} and ν_{16} are calculated to be 614 and 580 cm^{-1} with the corresponding observed frequencies 581 cm^{-1} [19] and ~565 cm^{-1} [17,19]. The planar-ring deformation mode ν_{17} and the non-planar ring deformation modes ν_{20} are correlated to the experimentally observed IR frequencies 567 and 683 cm^{-1} respectively.

C=O modes (3 modes)

The C=O group gives rise to three normal modes of vibration as a C=O stretching (ν), a C=O in-plane bending (β) and a C=O out-of-plane bending (γ) modes. The modes ν_{46}, ν_{21} and ν_{19} correspond respectively, to these modes. The present calculation shows that the C=O stretching mode (ν_{46}) with the calculated frequency at 1836 cm^{-1} having strong IR intensity and weak Raman intensity is strongly coupled with the ν(C=C) mode. The observed frequencies at ~1760 cm^{-1} with strong IR and weak Raman intensities were earlier [18, 19] correctly correlated to the ν(C=O) mode. The C=O in-plane bending vibration (β) is calculated to be 634 cm^{-1} (ν_{19}) with weak intensity in both the spectra with the corresponding observed frequency 621 cm^{-1}[19] and it is found to couple with the $\alpha(C_5\text{-}C_1\text{-}C_{12})$ mode. The C=O out-of-plane bending mode (γ) is found to have calculated frequency 751 cm^{-1} (ν_{21}) with the observed frequency 722 cm^{-1} [17, 19]. The presently observed IR frequencies 1755(vs) cm^{-1}, 630(m) cm^{-1} and 721(m) cm^{-1} are correlated to the modes ν_{46}, ν_{21} and ν_{19} respectively.

C-OH modes (12 modes)

Each of the two C-O(H) groups attached to the lactone ring has three normal modes as a ν{C-O(H)}, a β{C-O(H)} and a γ{C-O(H)} modes. However, for each of the two OH groups attached to the side chain, the two modes corresponding to the β{C-O(H)}and γ{C-O(H)} modes of the lactone ring OH groups become C-C-O angle deformation (α) and torsion (τ) of the CO(H) group about the C-C bond. Hence, the two OH groups attached to the side chain give rise

to the following six modes: $\nu\{C_{12}\text{-}O(H)\}$, $\nu\{C_{16}\text{-}O(H)\}$, $\alpha\{C_1\text{-}C_{12}\text{-}O(H)\}$, $\alpha\{C_{12}\text{-}C_{16}\text{-}O(H)\}$, $\tau\{C_1\text{-}C_{12}\text{-}O(H)\}$ and $\tau\{C_{12}\text{-}C_{16}\text{-}O(H)\}$.

The $\nu(C_4\text{-}OH)$ mode (ν_{37}) coupled with the $\alpha(C_5\text{-}O\text{-}H)$ and $\omega(CH_2)$ modes is calculated to be 1331 cm^{-1} with the corresponding observed IR and Raman frequencies ~1320 cm^{-1} [19]. The $\nu(C_5\text{-}OH)$ mode (ν_{32}) is calculated to be 1172 cm^{-1} corresponding to the observed frequency ~1140 cm^{-1} [17, 19] and appears to be strongly coupled with the $\alpha(C_4\text{-}O\text{-}H)$ mode. The $\nu(C_{12}\text{-}OH)$ mode (ν_{31}) does not appear to couple with any other mode(s) and could be correlated to the observed IR frequency 1121 cm^{-1} [19]. The mode ν_{29} arising due to the C_{16}-OH stretching vibration is calculated to be 1084 cm^{-1} with the corresponding observed frequency at ~1080 cm^{-1} [19]. The IR frequencies observed in the present case corresponding to the modes ν_{37}, ν_{32}, ν_{31} and ν_{29} are 1321, 1136, 1119 and 1072 cm^{-1} respectively.

Out of the two planar modes $\beta(C_4\text{-}OH)$ (ν_6) and $\beta(C_5\text{-}OH)$ (ν_9) calculated to be at 230 and 307 cm^{-1} the former could be correlated to the observed frequency 180 cm^{-1} [17] but no observed frequency could be correlated to the latter fundamental. The $\gamma(C_4\text{-}OH)$ mode (ν_{10}) is calculated to be 330 cm^{-1} and it is found to strongly couple with the $\gamma(C_5\text{-}OH)$ and $\alpha(C_1\text{-}C_{12}\text{-}H_{13})$ modes. No observed frequency could be correlated to this mode. The calculated frequency 148 cm^{-1} corresponding to the $\gamma(C_5\text{-}OH)$ mode (ν_4) is found to have weak IR and Raman intensities and the observed Raman frequency 122 (w) cm^{-1} [19] could be correlated to this mode.

The calculated frequency 280 cm^{-1} having weak IR and Raman intensities corresponding to the $\alpha(C_1\text{-}C_{12}\text{-}O_{14})$ mode (ν_8) is correlated to the observed Raman frequency 273(w) cm^{-1} [17] which also agrees with the presently observed IR frequency 273 cm^{-1}. The $\alpha(C_{12}\text{-}C_{16}\text{-}O_{19})$ mode (ν_7) is calculated frequency 255 cm^{-1} with the corresponding observed Raman frequency 238 (m) cm^{-1} [17]. The calculated frequencies 59 and 160 cm^{-1} correspond to the torsional modes (ν_1 and ν_5) about the $C_1\text{-}C_{12}$ and $C_{12}\text{-}C_{16}$ bonds with the former mode observed at 43 (vw) cm^{-1} in the Raman spectrum [17]. In the present case the experimentally IR band observed at 163 cm^{-1} with weak intensity is correlated to the latter torsional mode ν_5.

$C_1\text{-}C_{12}/C_{12}\text{-}C_{16}$ modes (6 modes)

The 6 normal modes of vibration arising due to the $C_1\text{-}C_{12}$ and $C_{12}\text{-}C_{16}$ bonds are: the two ν(C-C) and four δ(C-C) modes. The calculated frequencies 839 (ν_{24}) and 930 (ν_{25}) cm^{-1} correspond to the $\nu(C_1\text{-}C_{12})$ and $\nu(C_{12}\text{-}C_{16})$ modes the latter of which corresponds to the observed frequency 871 cm^{-1} [19] while no observed frequency could be correlated to the former mode. The experimentally observed IR frequency 868 cm^{-1} corresponds to the $\nu(C_{12}\text{-}C_{16})$ mode. The two δ modes (ν_{22} and ν_2) due to the $C_1\text{-}C_{12}$ bond are calculated to have the frequencies 777 and 79 cm^{-1} with the corresponding observed frequencies ~750 cm^{-1} [19] and 91(m) cm^{-1} [17]. In the present case the IR band at 757 cm^{-1} observed with strong intensity could be assigned to the mode ν_{22}. The former of the above two modes is strongly coupled with one of the ϕ(ring) modes. The remaining two δ modes (ν_{12} and ν_3) arising due to the $C_{12}\text{-}C_{16}$ bond have calculated frequencies 368 and 118 cm^{-1}, which could be correlated to the observed frequencies 340 and 113 cm^{-1} [17].

Comparison of vibrational modes of the molecular ions with the neutral molecule

The conversion of the L-AA molecule into its radical ions leads to significant increase in the Raman activities for all the O-H stretching modes (ν_{54}, ν_{53}, ν_{52} and ν_{51}), whereas the IR intensities increase for all the four O-H stretching modes in radical cation but in radical anion the IR intensities increase only for three O-H stretching modes. Further, the frequency for the ν(O-H) modes ν_{54} and ν_{53} shifts towards the lower wavenumber side in going from the neutral molecule to radical anion whereas further increase in going from the radical anion to the radical cation species. The magnitude of the calculated frequencies for the τ(O-H) modes ν_{14}, ν_{13} and ν_{11} increase in going from L-AA to L-AA$^-$ to L-AA$^+$. The present calculations show that the frequency for the OH torsional mode ν_{15} decreases for L-AA$^-$ by ~220 cm^{-1} and for L-AA$^+$ by ~213 cm^{-1}. The frequency for the α(C_{16}-O-H) mode ν_{42} is found to increase from 1431 cm^{-1} to 1460 cm^{-1} in going from the neutral species to the anionic species while it is found to reduce from 1460 cm^{-1} to 1383 cm^{-1} in going from the anionic species to the cationic species. Similarly, the frequency for the mode α(C_5-O-H) (ν_{43}) increases by ~86 cm^{-1} for the radical cation while it decreases by ~59 cm^{-1} for the radical anion as compared to the neutral molecule.

The ν_{as}(CH_2) mode (ν_{50}) is found to decreased in frequency by 47 cm^{-1} for L-AA$^-$ as compared to the neutral molecule however, it has nearly the same frequency for L-AA$^+$. The frequency for the ν_s(CH_2) mode (ν_{47}) decreases from 3011 cm^{-1} to 2943 cm^{-1} in going from L-AA to L-AA$^-$ and increases from 2943 cm^{-1} to 3051 cm^{-1} in going from L-AA$^-$ to L-AA$^+$. For the same vibrational mode (ν_{47}), the Raman activity increases significantly for L-AA$^+$ as a result of radicalization. In going from the L-AA$^-$ to L-AA$^+$ species, the Raman activities decrease significantly for the modes ν_{26} and ν_{33}. It is also found that the frequency corresponding to the τ(CH_2) mode (ν_{33}) increases by ~48 cm^{-1} for L-AA$^-$ and decreases by ~125 cm^{-1} for L-AA$^+$ as compared to the neutral molecule. The frequency corresponding to the mode (ν_{39}) is found to reduce from 1374 cm^{-1} to 1348 cm^{-1} in going from neutral to anionic species and increase from 1348 cm^{-1} to 1403 cm^{-1} in going from the anionic to cationic species.

The magnitudes of the frequencies of the C-H stretching modes ν_{49} and ν_{48} decrease by 18 and 211 cm^{-1} in going from the neutral to anionic species whereas these increase by 6 and 53 cm^{-1} in going from neutral to cationic species. The magnitudes of the calculated frequencies for the δ(C_{12}-H_{13}) modes ν_{38} and ν_{34} decrease by 37 and 27 cm^{-1} for L-AA$^-$ whereas increase by 15 and 33 cm^{-1} for L-AA$^+$ with respect to the neutral molecule. The calculated frequencies for the deformation modes of the C_1-H_{11} bond (ν_{40} and ν_{36}) decrease in going from the L-AA to L-AA$^-$ to L-AA$^+$ species.

Significant changes in the vibrational characteristics (magnitudes, intensities and depolarization ratios) of the C=C stretching mode ν_{45} accompanying the radicalization have been noticed. The other four ring stretching modes (ν_{30}, ν_{28}, ν_{27} and ν_{23}) are found to have decreased magnitude in going from L-AA to L-AA$^-$ while these are found to have increased magnitude in going from L-AA$^-$ to L-AA$^+$. The frequency of one (ν_{16}) of the two ring in-plane bending modes shifts towards the lower wavenumber side by 199 cm^{-1} for L-AA$^-$ and towards the higher wavenumber side by 11 cm^{-1} for L-AA$^+$ as compared to the neutral molecule. The two non-planar ring deformation modes (ν_{17} and ν_{18}) are found to have decreased frequencies by 265 and 264 cm^{-1} for L-AA$^-$ and increased frequencies by 45 and 139 cm^{-1} for L-AA$^+$.

The C=O stretching frequency (ν_{46}) decreases by 151 cm^{-1} in going from the neutral to the anionic species whereas it increases by 151 cm^{-1} in going from the anionic to the cationic species. For the above vibrational mode, the Raman activity increases significantly for the anionic and cationic species. It can also be seen (Table-3) that the calculated frequency for the out-of-plane deformation of C=O (ν_{21}) decreases in going from L-AA to $L\text{-}AA^+$ to $L\text{-}AA^-$ due to the radicalization process. It is observed that the IR intensity and Raman activity increase for the $L\text{-}AA^-$ due to the conversion process. However, the C=O in-plane bending mode (ν_{19}) frequency decreases in going from L-AA to $L\text{-}AA^-$ by ~68 cm^{-1}, while its magnitude is nearly same for the L-AA and $L\text{-}AA^+$ species.

The conversion of the neutral molecule shifts the magnitude of the frequency of the $\nu(C_5\text{-OH})$ mode ν_{32} by ~30 and 20 cm^{-1} towards lower wavenumber side for $L\text{-}AA^-$ and $L\text{-}AA^+$ and the IR intensity for the above frequency decreases in going from L-AA to $L\text{-}AA^-$ to $L\text{-}AA^+$. For the neutral L-AA molecule changes in the magnitude of the frequencies due to the ν(C-OH) modes ν_{37}, ν_{31} and ν_{29} are found to be insignificant while for the $L\text{-}AA^-$ molecule, the Raman activities are much more pronounced due to radicalization. The neutral L-AA molecule and its radical cation have nearly the same magnitude (~300 cm^{-1} and ~ 235 cm^{-1}) for both the β(C-OH) modes (ν_9 and ν_6). However, for the anion species the corresponding mode frequency decreases by ~40 cm^{-1} and ~90 cm^{-1} as compared to both the neutral and cationic species. The frequency of one (ν_{10}) of the two γ(C-OH) modes shifts towards lower wavenumber side by 13 cm^{-1} for $L\text{-}AA^+$ and by 34 cm^{-1} for $L\text{-}AA^-$ as compared to the neutral molecule. The frequencies corresponding to the $C_{12}\text{-}C_{13}\text{-}O_{19}/C_1\text{-}C_{12}\text{-}O_{14}$ angle bending modes ν_7 and ν_8 decrease by 34/36 cm^{-1} for $L\text{-}AA^-$ as compared to the neutral molecule, however it shifts upward by ~30/24 cm^{-1} in going from the $L\text{-}AA^-$ to $L\text{-}AA^+$ species. For both the τ(C-C) modes ν_1 and ν_5 relatively smaller changes are noted in the frequencies in going from the L-AA to $L\text{-}AA^-$ to $L\text{-}AA^+$ species.

For both the side chain C-C stretching modes significant changes are noticed in the Raman activities due to the radicalization process. Changes in the magnitudes of the frequencies corresponding to the δ(C-H) modes (ν_3 and ν_{22}) are found to be insignificant while the Raman activities are found to be enhanced for $L\text{-}AA^-$ as compared to the neutral and cationic species. The frequency corresponding to the C-H deformation mode ν_{12} shifts towards higher wavenumber side by ~230 cm^{-1} for $L\text{-}AA^-$ and by ~307 cm^{-1} for $L\text{-}AA^+$ with respect to the neutral molecule.

Table-3: Calculated and experimental fundamental frequencies[p] of L-AA and its radical ions

S. No.	L-AA Cal.	L-AA Exp.[q] FT-IR	L-AA Obs. a IR	L-AA Obs. a Raman	L-AA Obs. b IR	L-AA Obs. b Raman	L-AA Obs. c Raman	L-AA Obs. d IR	$L\text{-}AA^-$ Cal.	$L\text{-}AA^+$ Cal.	Mode[r]
ν_1	59 (0.98,0.47)	-	-	43vw	-	-	-	-	50 (0.16,54)	51 (3,48)	$\tau\{C_1\text{-}C_{12}\text{-}O(H)\}$

	0.74								0.09	0.38	
ν_2	79 (1,1) 0.72	-	-	91m	-	-	-	-	75 (1,11) 0.65	64 (4,1) 0.75	$\delta(C_1\text{-}C_{12})$
ν_3	118 (4,0.60) 0.75	-	-	113w	-	-	-	-	123 (17,851) 0.21	97 (8,0.46) 0.35	$\delta(C_{12}\text{-}C_{16})$
ν_4	148 (2,0.14) 0.50	-	-	122w	-	-	-	-	143 (64, 1094) 0.40	143 (2,40) 0.36	$\gamma(C_5\text{-OH})$
ν_5	160 (8,0.50) 0.75	-	-	-	-	-	-		136 (5, 673) 0.21	125 (3,10) 0.43	$\tau\{C_{12}\text{-}C_{16}\text{-O(H)}\}$
ν_6	230 (9,0.91) 0.70	-	-	180w	-	-	-	-	151 (28,38) 0.67	235 (13,1) 0.66	$\beta(C_4\text{-OH})$
ν_7	255 (4,0.39) 0.71	-	238m	-	-	-	237w	-	221 (12, 130) 0.22	251 (1,19) 0.42	$\alpha\{C_{12}\text{-}C_{16}\text{-O(H)}\}$
ν_8	280 (0.60,0.73) 0.07	273w	-	273w	-	-	-	-	244 (0.71,427) 0.12	268 (2,101) 0.30	$\alpha\{C_1\text{-}C_{12}\text{-O(H)}\}$
ν_9	307 (14,0.47) 0.32	-	-	-	-	-	-	-	260 (22,26) 0.55	297 (55,0.26) 0.62	$\beta(C_5\text{-OH})$
ν_{10}	330 (2,0.13) 0.67	-	-	-	-	-	318w	-	296 (82,1367) 0.06	317 (4,11) 0.41	$\gamma(C_4\text{-OH})$
ν_{11}	357 (161,1) 0.74	356vs	350s	-	-	-	-	-	587 (44,910) 0.14	664 (130,42) 0.40	$\tau(O_7\text{-}H_8)$
ν_{12}	368 (13,0.89) 0.74	-	340w	-	-	-	-	-	515 (11,290) 0.15	576 (21,240) 0.40	$\delta(C_{12}\text{-}C_{16})$
ν_{13}	420 (51,0.97) 0.09	-	366s	-	-	-	-	-	545 (29,1661) 0.06	602 (128,49) 0.22	$\tau(O_9\text{-}H_{10})$
ν_{14}	424	447m	-	-	-	-	-	-	447	566	$\tau(O_{14}\text{-}H_{15})$

(84,0.77) 0.75								(82,11436) 0.11	(112,3) 0.58	
ν_{15} 524 (25,3) 0.41	494vw	-	-	-	-	-	-	304 (14,298) 0.07	351 (88,55) 0.31	$\tau(O_{19}\text{-}H_{20})$
ν_{16} 564 (29,3) 0.56	-	-	-	-	-	-	-	365 (33,1666) 0.11	553 (7,2) 0.44	α(ring)
ν_{17} 580 (93,2) 0.21	567m	565m	-	-	564m	-	-	315 (55,955) 0.06	360 (31,1) 0.71	ϕ(ring)
ν_{18} 614 (128,5) 0.73	-	-	-	-	581w	588w	-	350 (9,303) 0.05	489 (19,212) 0.33	ϕ(ring)
ν_{19} 634 (3,9) 0.11	630m	-	-	-	621s	-	-	566 (90,4331) 0.07	631 (18,5) 0.38	β(C=O)
ν_{20} 693 (5,6) 0.17	683m	711vw	-	686w	693m	-	-	680 (18,958) 0.07	684 (20,75) 0.22	α(ring)
ν_{21} 751 (16,0.78) 0.14	721m	721m	-	722w	-	-	-	631 (32,14) 0.75	736 (7,43) 0.30	γ(C=O)
ν_{22} 777 (3,2) 0.13	757s	-	-	757s	742sh	-	-	750 (99,14669) 0.08	768 (6,19) 0.34	$\delta(C_1\text{-}C_{12})$
ν_{23} 830 (12,5) 0.63	822m	820m	-	821m	823m	828m	-	790 (29,2681) 0.08	813 (10,201) 0.38	ν(ring)
ν_{24} 839 (29,4) 0.59	-	-	-	-	-	-	-	837 (43,484) 0.16	833 (12,44) 0.19	$\nu(C_1\text{-}C_{12})$
ν_{25} 930 (13,5) 0.32	868m	869m	-	871w	871m	884w	-	898 (36,774) 0.04	920 (28,14) 0.57	$\nu(C_{12}\text{-}C_{16})$
ν_{26} 964 (26,2) 0.68	987vs	-	-	990s	-	946w	-	950 (71,1046) 0.06	961 (55,252) 0.35	$\rho(CH_2)$

ν_{27}	1038 (22,1) 0.35	1026vs	1025s	-	1027vvs	-	-	-	982 (66,656) 0.70	1005 (83,438) 0.41	ν(ring)
ν_{28}	1048 (78,0.58) 0.67	-	-	-	1046m	1048m	-	1045w	1013 (84,1480) 0.15	1032 (158,420) 0.31	ν(ring)
ν_{29}	1084 (26,4) 0.47	1072m	1074m	-	1077m	1081w	1061w	1075w	1102 (42,1471) 0.06	1075 (69,206) 0.40	ν(C_{16}-OH)
ν_{30}	1112 (274,9) 0.44	-	1118s	-	1113vs	1113s	-	-	1073 (151,1246) 0.05	1146 (222,165) 0.23	ν(ring)
ν_{31}	1116 (113,5) 0.61	1119s	-	-	1121vs	-	-	1118s	1123 (93,594) 0.21	1064 (59,461) 0.33	ν(C_{12}-OH)
ν_{32}	1172 (113,8) 0.41	1136m	1138s	-	1142vs	-	1153w	1139s	1142 (36,4415) 0.0021	1122 (17,13) 0.71	ν(C_5-OH)
ν_{33}	1221 (24,5) 0.73	1198m	1197m	-	1199s	1193w	-	1198m	1269 (28,1967) 0.05	1196 (29,139) 0.36	τ(CH_2)
ν_{34}	1240 (10,11) 0.60	1221m	1220m	-	1222s	-	1225w	1221m	1213 (64,461) 0.24	1273 (8,22) 0.27	δ(C_{12}-H_{13})
ν_{35}	1302 (99,2) 0.50	-	-	-	1246m	1258s	-	-	1247 (107,767) 0.06	1344 (118,2) 0.470	α(C_4-O-H)
ν_{36}	1314 (119,8) 0.65	1273m	1275m	-	1277s	-	-	-	1240 (9,614) 0.59	1230 (74,129) 0.33	δ(C_1-H_{11})
ν_{37}	1331 (101,14) 0.29	1321vs	1320s	-	1322s	1323s	1300w	1321s	1297 (52,5031) 0.05	1361 (56,127) 0.21	ν(C_4-OH)
ν_{38}	1364 (15,3) 0.27	-	-	1344vw	-	-	-	-	1327 (14,799) 0.14	1372 (81,8) 0.30	δ(C_{12}-H_{13})
ν_{39}	1374 (4,8) 0.22	1361m	1362m	-	1364m	-	1361w	-	1348 (58,5086) 0.05	1403 (22,32) 0.25	ω(CH_2)

ν_{40}	1388 (10,4) 0.53	-	-	1372w	-	1371w	-	-	1382 (32,4009) 0.05	1310 (113,3) 0.61	$\delta(C_1\text{-}H_{11})$
ν_{41}	1415 (39,4) 0.67	1388m	-	-	1389m	-	-	-	1415 (30,43) 0.03	1417 (58,66) 0.25	$\alpha(C_{12}\text{-}O\text{-}H)$
ν_{42}	1431 (41,5) 0.31	-	1385m	-	-	-	-	-	1460 (51,10) 0.43	1383 (13,5) 0.50	$\alpha(C_{16}\text{-}O\text{-}H)$
ν_{43}	1448 (50,7) 0.52	1443m	1435m	-	-	-	-	-	1389 (66,1961) 0.09	1534 (138,60) 0.29	$\alpha(C_5\text{-}O\text{-}H)$
ν_{44}	1501 (6,6) 0.75	1492w	1482w	1482w	1487m	1484m	1477w	-	1495 (188,60) 0.31	1493 (3,155) 0.39	$\sigma(CH_2)$
ν_{45}	1769 (478,96) 0.16	1674vvs	1670vs	1670vs	1675vvs	1661vvs	1699 vvs	1672vs	1557 (8,3674) 0.04	1707 (116,2103) 0.34	$\nu(C=C)$
ν_{46}	1836 (367,20) 0.34	1755vs	1753s	1753w	1764s	1758w	1765w	1755m	1685 (1825,35699) 0.05	1836 (333,271) 0.14	$\nu(C=O)$
ν_{47}	3011 (33,76) 0.15	-	-	-	-	2879wsh	-	-	2943 (80,88) 0.60	3051 (22,211) 0.06	$\nu_s(CH_2)$
ν_{48}	3034 (7,88) 0.45	2917m	2915m	2915vs	2917m	2919s	2956s	-	2823 (265,5593) 0.41	3087 (4,115) 0.29	$\nu(C_1\text{-}H_{11})$
ν_{49}	3046 (46,184) 0.12	-	-	-	2907m	-	-	-	3028 (23,79) 0.68	3041 (3,67) 0.75	$\nu(C_{12}\text{-}H_{13})$
ν_{50}	3100 (22,130) 0.37	3036s	-	-	3030sbr	3004w	-	-	3053 (1182,69) 0.71	3104 (7,700) 0.35	$\nu_{as}(CH_2)$
ν_{51}	3744 (72,42) 0.06	3220vs	3230m	-	3216s	-	-	-	3788 (32,74) 0.53	3670 (167,93) 0.66	$\nu(O_{14}\text{-}H_{15})$
ν_{52}	3767 (118,83) 0.19	3317vs	3330s	-	3315s	-	-	-	3746 (32,1578) 0.21	3601 (305,1383) 0.73	$\nu(O_7\text{-}H_8)$

ν_{53}	3779 (87,41) 0.15	3412vs	3420s	-	3410s	-	-	-	3696 (205,1185) 0.07	3829 (68,472) 0.19	$\nu(O_{19}\text{-}H_{20})$
ν_{54}	3798 (109,101) 0.23	3528vs	3535s	-	3626s	-	-	-	3529 (67,25357) 0.48	3685 (278,144) 0.66	$\nu(O_9\text{-}H_{10})$

p: The first and second numbers within each bracket represent IR intensity(Km/mol) and Raman activity($\AA^4$/amu) while
the number above and below each bracket represent the corresponding calculated frequency(cm^{-1}) and depolarization
ratios of the Raman band respectively.
s: strong, m: medium, w: weak, vs: very strong, vvs: very very strong. r: ν=stretching, ω=wagging, τ=twisting, ρ=rocking, σ=scissoring, δ= deformation, γ=out-of-plane deformation, β=in-plane deformation, α=angle bending, ν_s=symmetric stretching, ν_{as}= anti-symmetric stretching, α= in–plane ring bending, ϕ=out-of-plane ring bending. q: From solid state FT-IR spectra in KBr pellet and Far-IR spectra in Nujol mull.
a: ref.[27],b: ref.[29], c: ref.[30],d: ref.[31].

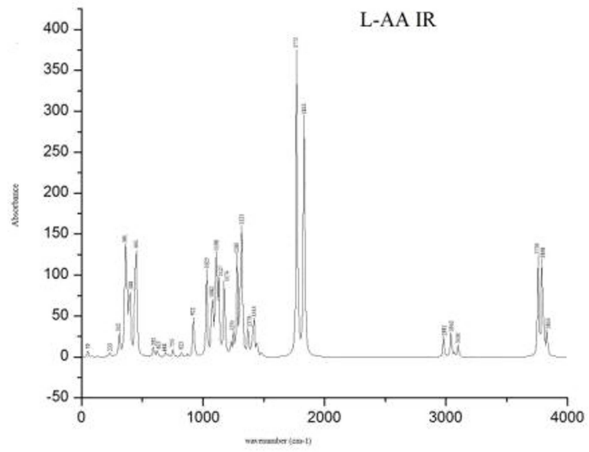

Fig.-8: Calculated IR spectrum of L-AA

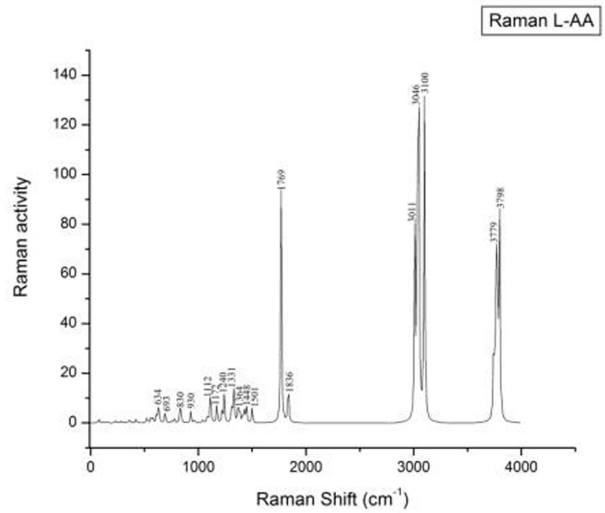

Fig.-9: Calculated Raman spectrum of L-AA

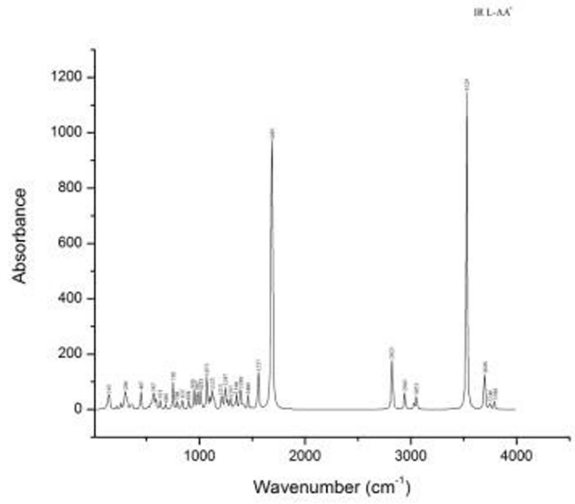

Fig.-10: Calculated IR spectrum of L-AA$^-$

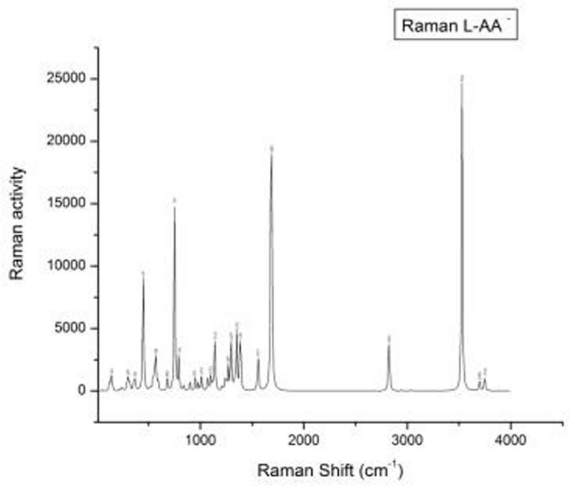

Fig.-11: Calculated Raman spectrum of L-AA$^-$

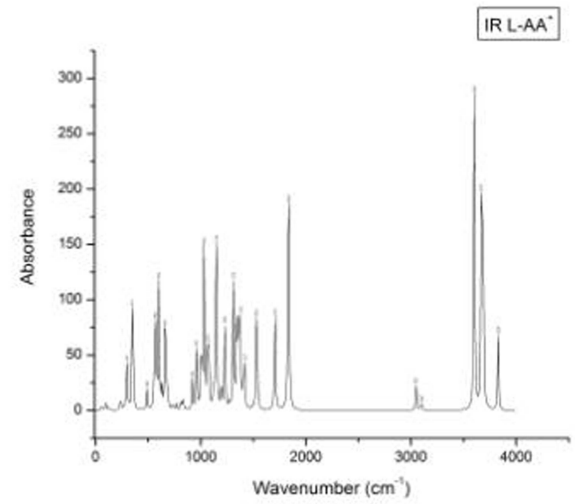

Fig.-12: Calculated IR spectrum of L-AA$^+$

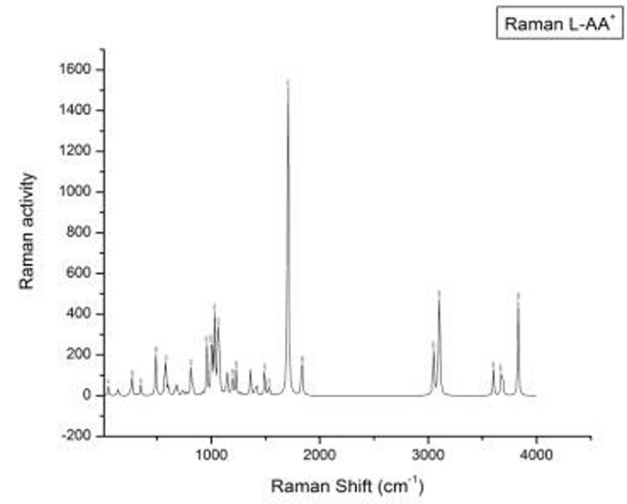

Fig.-13: Calculated Raman spectrum of L-AA$^+$

Figs. 8-13 : The calculated vibrational frequencies, IR intensity and Raman activity of L-AA and its radical ions

Thermodynamics properties

The molar heat capacity (C_V) at constant volume, entropy (S), thermal energy (TE) and zero-point vibrational energy (ZPVE), total energy (E) and dipole moment (μ) were obtained for the neutral L-AA molecule and its radical anionic and cationic species and these are collected in the Table-4. The calculated dipole moment decreases in going from the L-AA and L-AA$^-$ species. The radical anion is calculated to have lower energies compared to both the neutral and anionic species.

Table – 4: Calculated Energies, Dipole Moments and Thermodynamic Functions^r for the L-AA and its radical ions

S. No.	Species	Total Energy (E)	Zero-point vibrational energy (ZPVE)	Dipole Moment (μ)	Constant volume molar heat capacity (C_V)	Entropy (S)	Thermal Energy (TE)
1	**L-AA**	-684.993	394852.1	3.325	43.063	105.055	101.622
2	**L-AA$^-$**	-684.998	380384.6	2.329	45.233	110.883	98.743
3	**L-AA$^+$**	-684.677	393123.5	6.072	42.784	107.543	101.222

r:E & ZPVE are measured in Hartrees & Joules/Mol respectively, C_V & S are measured in Cal/Mol-Kelvin, TE is measured in Kcal/Mol.

CONCLUSION

In the L-AA molecule shortening of the r(C_3-C_4) bond by 0.042 Å as compared to the r(C_1-C_5) bond is due to attachment of an O atom at the site C_3. The carbonyl bond lengths r(C_4-O_7) and r(C_5-O_9) for L-AA$^-$ are increased whereas for L-AA$^+$ these are found to be decrease as compared to the neutral molecule. The bond angles α(O_2-C_1-C_{12}), α(H_{11}-C_1-C_{12}) and α(O_2-C_3-O_6) for L-AA$^-$ increase but L-AA$^+$ decrease as compared to the neutral molecule whereas the bond angle α(O_2-C_3-C_4) decreases for the both radical ions as compared to the neutral molecule. The dihedral angle H_{13}-C_{12}-C_{16}-H_{18} increases by 12.4° while reverse effect is noticed for the dihedral angles C_1-C_{12}-C_{16}-O_{19} and H_{13}-C_{12}-C_{16}-H_{17} which decrease by 15.4° and 14.3° respectively, in going from L-AA to L-AA$^-$ while the value of the dihedral angles H_{13}-C_{12}-C_{16}-O_{19} and O_{14}-C_{12}-C_{13}-O_{19} increase by ~16° in going from the neutral molecule to anionic species whereas these decrease by 27.8° in going from the anionic to cationic species. The APT charges at the sites O_{14} and O_{19} increase in going from the L-AA$^+$ to L-AA$^-$ and L-AA$^+$ to L-AA species. In the lactone ring, all the four C atoms possess positive charges but in L-AA$^-$, C_4 and C_5 are negative as these are hardly affected by bond character. The maximum positive charge is on the atom C_3 due to attachment of the two electronegative O atoms at the C_3 site. The charges at the sites C_{12} and C_{13} decrease by 0.0523 and 0.0261 in going from L-AA to L-AA$^-$ but increase by 0.0836 and 0.0187 in going from the L-AA$^-$ to L-AA$^+$ species.

All the 54 normal modes of the L-AA molecule have been assigned and discussed in details. It could be possible presently to correlate 47 normal modes to the experimentally observed IR/Raman frequencies. The CH_2 anti-symmetric (ν_{50}) and symmetric (ν_{47}) stretching modes (Table-3) do not couple with any other modes, except the C_1-H_{11} stretching mode which couples with the $\nu_s(CH_2)$ mode. The two δ modes (ν_{38} and ν_{34}) arising due to the C_{12}-H_{13} bond have calculated frequencies 1364 and 1240 cm^{-1} and are strongly coupled with the two δ(C_1-H_{11}) modes. The lowest ring stretching mode ν_{23} having the calculated frequency 825 cm^{-1} is strongly coupled with the α(ring) mode and similarly, the C=O stretching mode (ν_{46}) is strongly coupled with the ν(C=C) mode. The other planar-ring deformation mode ν_{17} appears to arise due to ring deformation strongly coupled with the τ(O_{15}-H_{16}) and τ(O_{19}-H_{20}) modes. The APT charges and complexity of hydrogen bonding in the lactone ring and the side chain lead to the magnitudes of the four OH stretching modes in the order ν(O_9-H_{10})>ν(O_{19}-H_{20})>ν(O_7-H_8)>ν(O_{15}-H_{16}) (Table-3 modes ν_{51}-ν_{54}) for the neutral molecule. The magnitudes of the frequencies of the C-H stretching modes ν_{49} and ν_{48} decrease by 18 and 211 cm^{-1} in going from the neutral to anionic species

whereas these increase by 6 and 53 cm^{-1} in going from the neutral to the cationic species. The magnitudes of the calculated frequencies for the $\delta(C_{12}\text{-}H_{13})$ modes ν_{38} and ν_{34} decrease by 37 and 27 cm^{-1} for L-AA^- while these increase by 15 and 33 cm^{-1} for L-AA^+ with respect to the neutral molecule. The radicalization of the neutral molecule shifts the magnitude of the frequency of the $\nu(C_5\text{-}OH)$ mode ν_{32} by ~30 and 20 cm^{-1} towards the lower wavenumber side for L-AA^- and L-AA^+ and the IR intensity for the above mode decreases in going from L-AA to L-AA^- to L-AA^+. The calculated dipole moment has the highest value for the L-AA^+ species and the lowest value for the neutral species. The radical anion is calculated to have lower energies compared to both the neutral and anionic species.

ACKNOWLEDGEMENTS

The author (Priyanka Singh) are thankful to Department of Chemistry, B. H. U., U.P. (India) for giving permission to use the FTIR spectrometer for getting recorded the FTIR spectra.

REFERENCES

[1] M Levine. *N. Engl. J. Med*., **1986**, 314, 892-902.
[2] I M. Lee. *Proc. Assoc. Am. Phys*., **1999**, 111, 10-15.
[3] A C Carr; B. Frei. *Am. J. Clin. Nutr*.,**1999**, 69, 1086-1107.
[4] R E Patterson;, E White; A R Kristal; M L Nuehouser; J D Potter. *Cancer Causes Contr*., **1997**, 8, 786-807.
[5] K. A. Head, *Altern. Med. Rev*.,**1998**, 3, 175-186.
[6] K N Prasad; A Kumar; V Kochu Pilla; W C Cole. *J. Am. Coll. Nutr*., **1999**, 18, 13-25.
[7] W. M. Cort, Antioxidant properties of ascorbic acid in foods, in: P.A. Seib, B. M. Tolbest(Eds.), Ascorbic Acid Chemistry, Metabolism and Uses, Adv. Chem. Ser. N. 200 P531, American Chemical Society, Washington, DC, **1982**.
[8] M J Barnes; E Kodicek. *Vitamins Hormones*., **1972,** 30, 1-43.
[9] L S Hollis; A R Amudsen; E W Stern. *J. Am. Chem. Soc.*, **1985**, 107, 274-276.
[10] C I Rivas; J C Vera; V H Guaiquil; F V Velasquez; O A Borquez-Ojeda; J G Carcamo; I I Concha; D W Golde. *J. Biol. Chem*., **1997**, 272, 5814-5820.
[11] J Hvoslef. *Acta Cryst*., **1968,** B24, 23-35.
[12] J Hvoslef. *Acta Cryst*.**1968,** B24, 1431-1440.
[13] J Hvoslef. *Acta Cryst*., **1969,** B25,2214-2223.
[14] M A Al-Laham; G A Petersson; P Haake. *J. Comp. Chem*., **1991**, 12, 113-118.
[15] M A Mora; F J Melendez. *J. Mol. Struct*., **1998**, 454,175-185.
[16] W Lohmann; D Pagel; V Penka. *Eur. J. Biochem*., **1984**, 138, 479-480.
[17] J Hvoslef; P K Laeboe. *Acta. Chem. Scand*., **1971**, 25, 3043-3053.
[18] Y Dimitrova. *Spectrochim. Acta* A, **2006**, 63, 42-437.
[19] C Y Panicker; H T Vargheseb; D Philip. *Spectrochim. Acta* A, **2006,** 65, 802-804.
[20] J T Edsall; E L Sagall. *J. Chem. Phys*., **1943**, 65, 1312-1316.
[21] E G Ferrer; E J Baran. *Bio. Tra. Ele. Rese*., **2001**, 83, 111-119.
[22] P Singh; N P Singh; R. A. Yadav. Author's unpublished work.
[23] M J Frisch; GW Trucks; HB Schlegel; G E Scuseria; M A Robb; J R Cheeseman; J A Montgomery Jr.; T Vreven; K N Kudin; J C Burant; J M Millam; S S Iyengar; J Tomasi; Barone; B Mennucci; M Cossi; G Scalmani; N Rega; G A Petersson; H Nakatsuji; M Hada; M Ehara; K

Toyota; R Fukuda; J Hasegawa; M Ishida; T Nakajima; Y Honda; O Kitao; H Nakai; M Klene; X. Li; J E Knox; H P Hratchian; J B Cross; C Adamo; J Jaramillo; R Gomperts; RE Stratmann; O Yazyev; A J Austin; R Cammi; C Pomelli; J W Ochterski; P Y Ayala; K Morokuma; G A Voth; P Salvador; J J Dannenberg; V G Zakrzewski; S Dapprich; A D Daniels; M C Strain; O Farkas; D K Malick; A D Rabuck; K Raghavachari; J B Foresman; J V Ortiz; Q Cui, A G Baboul; S Clifford; J Cioslowski; B B Stefanov; G Liu; A Liashenko; P Piskorz; I Komaromi; R L Martin; D J Fox; T Keith; M A Al-Laham; CY Peng; A Nanayakkara; M Challacombe; P M W Gill; B Johnson; W Chen; M W Wong; C Gonzalez and J A Pople. Gaussian 03, Revision C. 02, Gaussian, Inc., Wallingford, CT, **2004**.

[24] A Frisch; A B Nielson; A J Holder. GAUSSVIEW User Manual, Gaussian Inc.; Pittsburgh, PA, **2000**.